

# Modeling the creep deformation and damage evolution of superalloy GH4169: Application of a novel damage constitutive model based on continuum damage mechanics

Xu Zhao<sup>1</sup>, Xuming Niu<sup>1</sup>, Yingdong Song<sup>1</sup>, and Zhigang Sun<sup>1</sup>

<sup>1</sup>Nanjing University of Aeronautics and Astronautics

July 1, 2022

## Abstract

In order to accurately predict creep deformation and damage evolution of nickel-based superalloy GH4169, a novel damage constitutive model, which can be called TTC CDM-based model, was proposed based on TTC relations and continuum damage mechanics (CDM). The stress and temperature dependence of constants were all determined in the novel model, which overcame the weakness of the traditional CDM-based model and made the model have the satisfactory abilities of interpolation and extrapolation. Microstructural study has revealed that the creep fracture mode gradually converts from intergranular brittle fracture to transgranular ductile fracture as the stress decreases. And the critical conditions were identified. It was determined that the novel model accurately predicted the minimum creep rate, rupture time, creep deformation and damage evolution process of GH4169. Furthermore, the nonlinear creep damage accumulation effect was also revealed by the novel model, i.e. the total creep life of GH4169 will be reduced if high stress or high temperature condition was applied first, which was consistent with previous experimental results of variable creep load.

## Modeling the creep deformation and damage evolution of superalloy GH4169: Application of a novel damage constitutive model based on continuum damage mechanics

Xu Zhao<sup>a,b</sup>, Xuming Niu<sup>a,b</sup>, Yingdong Song<sup>a,b,c,\*</sup>, Zhigang Sun<sup>a,b,\*</sup>

<sup>a</sup> College of Energy & Power Engineering, Nanjing University of Aeronautics and Astronautics, Nanjing, 210016, China

<sup>b</sup> Key Laboratory of Aero Engine Thermal Environment and Thermal Structure, Ministry of Industry and Information Technology, Nanjing, 210016, China

<sup>c</sup> State Key Laboratory of Mechanics and Control of Mechanical Structures, Nanjing University of Aeronautics and Astronautics, Nanjing, 210016, China

\* Corresponding author. E-mail: szg\_mail@nuaa.edu.cn; ydsong@nuaa.edu.cn

## Abstract

In order to accurately predict creep deformation and damage evolution of nickel-based superalloy GH4169, a novel damage constitutive model, which can be called TTC CDM-based model, was proposed based on TTC relations and continuum damage mechanics (CDM). The stress and temperature dependence of constants were all determined in the novel model, which overcame the weakness of the traditional CDM-based model and made the model have the satisfactory abilities of interpolation and extrapolation. Microstructural study has revealed that the creep fracture mode gradually converts from intergranular brittle fracture to transgranular ductile fracture as the stress decreases. And the critical conditions were identified. It was determined

that the novel model accurately predicted the minimum creep rate, rupture time, creep deformation and damage evolution process of GH4169. Furthermore, the nonlinear creep damage accumulation effect was also revealed by the novel model, i.e. the total creep life of GH4169 will be reduced if high stress or high temperature condition was applied first, which was consistent with previous experimental results of variable creep load.

## Keywords

Damage constitutive model, continuum damage mechanics (CDM), damage evolution process, nonlinear creep damage accumulation effect

## Nomenclature

material constants	creep strain rate
fitting constants	the minimum creep rate
material constants	the final creep rate
the number of test data	constants which depend on stress and temperature
stress exponent of K-R model	applied stress
stress exponent of L-M model	material constants
material constants of L-M model	threshold stress
apparent activation energy	ultimate tensile strength
universal gas constant	damage
creep temperature	damage rate
rupture time	initial damage
normalized time of 1 <sup>st</sup> step load	the analytical damage
normalized time of 2 <sup>nd</sup> step load	the experimental damage
initial time	

## 1. Introduction

Due to the increasing requirements of low carbon emission and high efficiency, creep failure has become one of the most important failure modes for many engineering components, such as gas turbine, aero-engine, and power generation system, etc. Therefore, the ability to accurately evaluate and predict the creep behavior is of great importance for the integrity of high temperature structure. The typical creep deformation curve can be defined in three distinct stages, i.e. primary, secondary, and tertiary stages<sup>1</sup>. In the primary stage, with the increase of time-dependence creep deformation, the work hardening occurs gradually, the mobile dislocation density and the creep strain rate decrease with time<sup>2</sup>. When the creep rate reaches to the minimum value, creep enters the secondary stage. With further development of deformation, the onset of tertiary creep occurs. Dislocations gradually pill up at defects, such as grain boundaries and second-phase particles, which lead to stress concentration. And the cavities gradually nucleate at the location of stress concentration, then grow up and coalesce into macro-cracks<sup>3-5</sup>. Finally, it results in the fracture of the material.

It is obvious that the creep deformation is always accompanied by the damage evolution process, Dyson<sup>6</sup> identified three categories of creep damage: (1) strain-induced damage(including grain boundary cavitation, dynamic subgrain coarsening, and mobile dislocation multiplication); (2) thermal-induced damage(including coarsening of particles, and solute depletion); (3) environment-induced damage (including oxidation, sulphuration, and carbonization). In order to study the damage process, continuum damage mechanics (CDM) was developed by Kachanov<sup>7</sup> who introduced a continuity factor to reflect the degree of material degradation. Based on the creative work of Kachanov, Rabotnov<sup>8</sup> established the damage variable and defined the concept of effective stress. After that, Lemaitre<sup>9</sup>, Chaboche<sup>10</sup>, Krajcinovic<sup>11</sup>, and Murakami<sup>12</sup>, etc. further developed the continuum damage mechanics theory.

Continuum damage mechanics is a branch of damage mechanics, which is used to study the mechanical process of damage. And it can be divided into physically based damage constitutive model and empirically based damage constitutive model<sup>13</sup>. The former usually develops multiple damage variables to distinguish the effect of different damage mechanisms, and defines a damage variable separately for each damage mechanism. On the contrary, the latter defines a single empirical damage variable to quantify the material degradation caused by different damage mechanisms. In general, physically based damage constitutive model contains a large number of material parameters, which leads to many difficulties and inconveniences in engineering application. Because of the simplicity of the empirically based damage constitutive model, such as Kachanov-Rabotnov damage model, Liu-Murakami damage model and Sinh damage model, it has been widely used in practical applications. Hyde studied the creep behavior of notched P91 steel specimens by using Kachanov-Rabotnov damage model and Liu-Murakami damage model<sup>14</sup>. Guo investigated damage accumulation of manifold component and modified Liu-Murakami damage model<sup>15</sup>. Saberi utilized Liu-Murakami damage model to assess the life of blade-disk attachments<sup>16</sup>. Praveen<sup>17</sup> and Wang<sup>18</sup> used Kachanov-Rabotnov damage model to predict the creep damage behavior of 316LN steel and UNS N1003 alloy, respectively. Recently, a Sinh damage model was proposed by Haque<sup>19</sup>, and some comparative analysis of Sinh and Kachanov-Rabotnov damage models can also be found in available published literatures<sup>20–22</sup>.

However, it is worth noting that the empirically based damage constitutive model is generally established on the basis of power-law equation and Sinh equation. It is difficult to reliably extrapolate the short-term creep data obtained under high stress and high temperature in laboratory condition to the long-term practical condition of engineering components, due to the lack of explicit stress and temperature dependence of the constants in above damage constitutive models. In order to achieve reasonable extrapolation, Cano<sup>23</sup> tried to combine the Wilshire equations with the damage constitutive model. However, the adopted region-splitting method was contrary to the original intention of Wilshire and made the model more complex<sup>24–27</sup>.

Our latest research results<sup>28</sup> showed that intrinsic relations exist between threshold stress, tensile properties and creep behavior, and the TTC relations were proposed, which were better at predicting the creep behavior than Wilshire equations. Therefore, to ensure the accuracy of extrapolation of long-term creep behavior, a novel damage constitutive model was derived which combines the TTC relations with continuum damage mechanics. Post-audit validation was also conducted to verify the predictive ability of the novel model, and it was determined that the model displays satisfactory predictive results. Interestingly, the nonlinear creep damage accumulation effect was revealed by the novel model, which was consistent with our previous experimental results<sup>29</sup>. And this phenomenon further showed the accuracy of the damage constitutive model from the aspect of damage accumulation process.

## 2. The existing creep damage constitutive models

### 2.1. Kachanov-Rabotnov damage model

Continuum damage mechanics (CDM) was first developed by Kachanov<sup>7</sup>, and then extended by Rabotnov<sup>8</sup>. The Kachanov-Rabotnov damage model, also known as K-R model can be expressed as:

where  $\dot{\epsilon}$  is creep strain rate,  $D$  is the damage ranging from 0 to 1,  $\dot{D}$  is creep damage rate,  $\sigma$  is the applied stress,  $n$  is the stress exponent, and  $A, B$  are the material constants. When  $D = 1$ , failure occurs. The K-R model assumes that the damage mainly occurs in the tertiary stage, i.e. damage is zero before entering the tertiary stage. Hence when Eq. (1) can be written as:

where  $\dot{\epsilon}_0$  is the minimum creep strain rate. It can be seen that the K-R model is essentially based on the power-law equation. There are five material constants are required to define in the K-R model, and several constant determination methods have been proposed by different researchers<sup>30–32</sup>.

### 2.2. Liu-Murakami damage model

Liu and Murakami pointed out that significant damage localization and mesh-dependence of K-R model

could be found when used in FE analysis<sup>33</sup>. This can be attributed to the damage term in the denominator. As the damage approaches to unity, the strain rate and damage rate will approach to infinity, due to the terms and in Eq. and Eq., respectively. Therefore, the exponential form of damage constitutive model was proposed by Liu and Murakami<sup>33</sup>:

where  $n$  is the stress exponent, and  $A$ ,  $B$ , and  $C$  are the material constants. Research results of copper showed that the great improvements in damage localization and mesh-dependence were achieved by the Liu-Murakami model<sup>34</sup>.

### 2.3. Sinh damage model

Both the K-R model and the Liu-Murakami model are established on the basis of the power-law equation. The characteristics of the stress exponent changing with stress and temperature limit their applications. To overcome the limitation of power-law equation, Haque and Stewart proposed the Sinh damage constitutive model<sup>20</sup>:

where  $A$  and  $B$  are the secondary creep stage constants which can be obtained from the minimum creep rate equation  $\dot{\epsilon}_m = A \sigma^m \exp(-Q/RT)$ , and  $C$ ,  $D$ , and  $E$  are material constants. To ensure when failure occurs, constant  $F$  is defined as  $F = \dot{\epsilon}_f / \dot{\epsilon}_m$ , where  $\dot{\epsilon}_f$  is the final creep rate when specimen fracture, which can be determined directly from the experimental data.

It can be observed that the above damage models are essentially based on the power-law equation and Sinh equation. The undetermined stress and temperature dependence of related parameters make it difficult to achieve reliable extrapolation. Therefore, most of the published literatures aimed to model the creep behavior within a certain stress range and at a single temperature<sup>17,35-37</sup>. This means that it is very challenging to extrapolate the short-term creep data obtained in the laboratory to the long-term practical service. It is necessary to develop a novel damage constitutive model to achieve reliable extrapolation, in which all parameters have clear stress and temperature dependence.

### 3. A novel damage constitutive model based on TTC relations

In recent investigation<sup>28</sup>, the intrinsic relations between threshold stress, tensile properties, and creep behavior were established. These relations, called TTC relations, can be expressed as

where  $\sigma_0$ ,  $\sigma_u$ , and  $\dot{\epsilon}_m$  are constants,  $\sigma_0$  is the threshold stress,  $\sigma_u$  is the ultimate tensile strength,  $\dot{\epsilon}_m$  is the minimum creep rate,  $R$  is the gas constant ( $J/mol \cdot K$ ),  $t_r$  is rupture time, and  $Q$  is the apparent activation energy of TTC relations which can be calculated at constant  $\dot{\epsilon}$ . Rearranging Eq. and Eq. to obtain and as follows

TTC relations are established on the basis of assumption that  $\sigma_0$  and  $\sigma_u$  as  $\sigma_0 = \sigma_u - \Delta\sigma$ , while  $\dot{\epsilon}_m$  and  $\dot{\epsilon}_f$  as  $\dot{\epsilon}_m = \dot{\epsilon}_f / F$  according to threshold stress theory<sup>38-40</sup>. Combining the TTC relations with continuum damage mechanics (CDM), a novel damage constitutive model, called TTC CDM-based model can be derived as

where  $\dot{\epsilon}$  is creep strain rate,  $D$  is damage ( $0 \leq D < 1$ ),  $\dot{D}$  is damage rate, and  $A$ ,  $B$ , and  $C$  are parameters which depend on stress and temperature. To ensure when failure occurs, the constant  $F$  is also defined as

where  $\dot{\epsilon}_f$  is the final creep rate, which can be determined directly from experimental data. Introducing constant  $F$  into Eq., the experimental damage takes the form

Integration of damage evolution Eq. with assumption of initial time and initial damage  $D_0$ , the analytical damage takes the form

when  $\sigma$ ,  $\dot{\epsilon}$ . The constant controls the curvature of damage evolution curve, which can be determined by least square fitting of experimental damage Eq. and analytical damage Eq..

#### 4. Experimental procedures

In order to validate the predictive ability of the novel damage constitutive model, creep experiments of nickel-based superalloy GH4169 were conducted. The creep specimens with 26.6mm gauge length and 5 mm gauge diameter were fabricated from 22 mm as-received cylindrical bars. The creep tests were performed under stress range of 515MPa-925MPa and temperature range of 600-650. The specific experimental details are listed in Table 1. Specimens 1-12 were used to calibrate the novel damage constitutive model. Furthermore, in order to verify the interpolation and extrapolation abilities of the model, specimens 13-18 were designed to perform the post-audit validation. It is worth noting that the experimental conditions of specimens 13-15 are the same as specimens 8-9. The purpose of this repeated trials is to further illustrate the scatter of the creep data.

After the creep experiments, the ruptured specimens at different temperature and stress levels were prepared for microstructural observation by using scanning electron microscope (SEM). The standard metallographic methods were adopted including grind, polish and etch.

TABLE 1 Experimental details of creep tests.

No.	/	/MPa	Note	No.	/	/MPa	Note
1	600	925	Calibration	10	650	670	Calibration
2		880		11		615	
3		850		12		595	
4		820		13	650	770	Interpolation
5		805		14		720	
6		790		15		720	
7	650	820	Calibration	16	650	515	Extrapolation
8		770		17	615	850	
9		720		18		820	

#### 5. Results

##### 5.1. Creep behavior analysis

The obtained creep curves are shown in Figure 1, and the obtained minimum creep rate and rupture time are summarized in Table 2. The rupture time varies from 17 hours to 942 hours, which increases with the decrease of the applied stress at the same temperature. It can be seen from specimens 8, 13, and specimens 9, 14, 15 that obvious scatter of creep data exists. The origin of the scatter comes from many sources, such as the fluctuation of test conditions, surface roughness, grain size and inhomogeneous microstructure<sup>41,42</sup>.

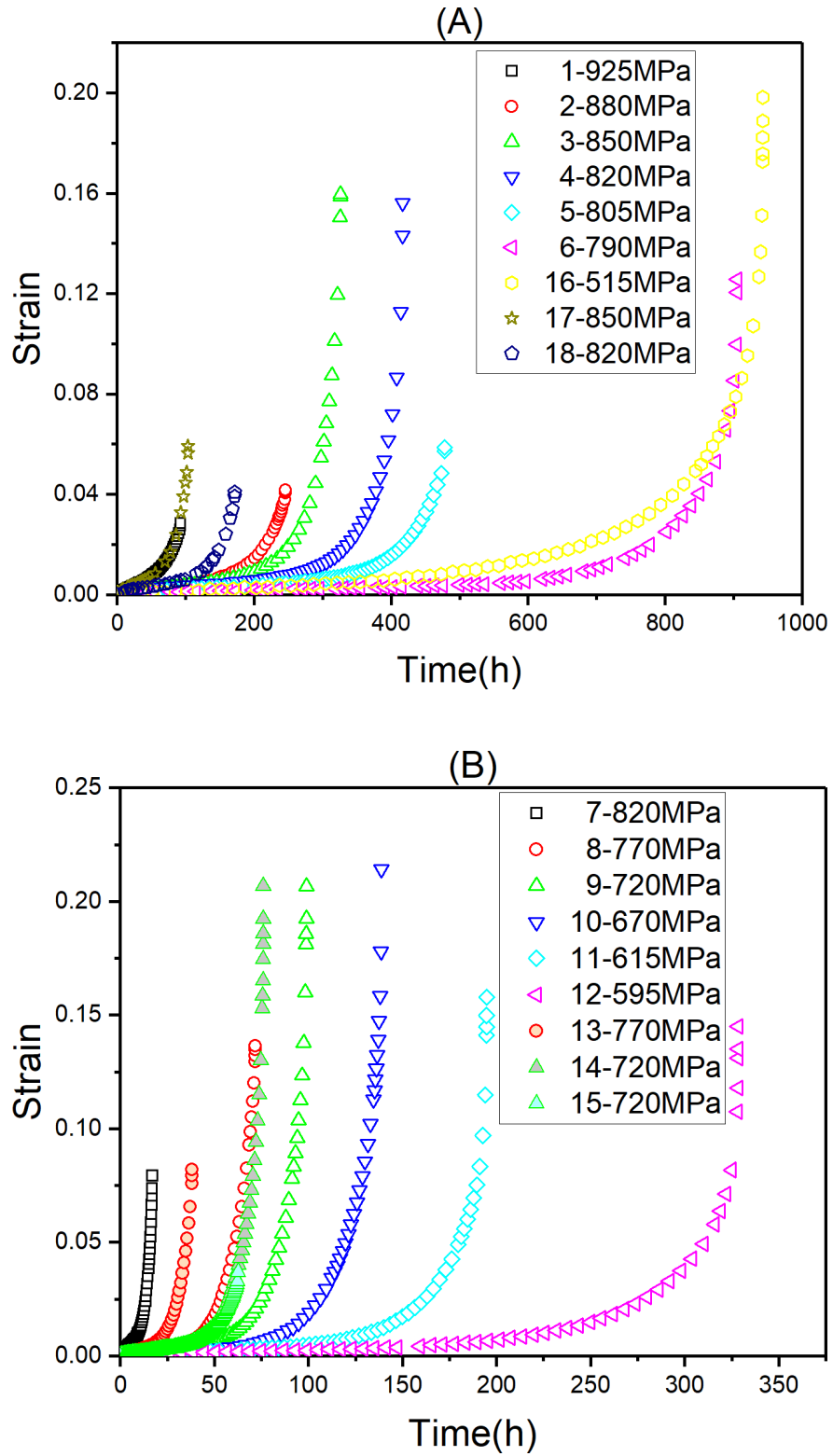


FIGURE 1 Creep curves of (A) specimens 1-6, 16-18, and (B) specimens 7-15.

TABLE 2 Experimental results of creep test.

No.	/	/MPa	/	/	No.	/	/MPa	/	/
1	600	925	$1.23 \times 10^{-4}$	92	10	650	670	$7.0 \times 10^{-5}$	139
2		880	$3.20 \times 10^{-5}$	246	11		615	$4.1 \times 10^{-5}$	195
3		850	$2.20 \times 10^{-5}$	326	12		595	$2.5 \times 10^{-5}$	328
4		820	$1.60 \times 10^{-5}$	416	13	650	770	$2.40 \times 10^{-4}$	38
5		805	$1.40 \times 10^{-5}$	478	14		720	$1.20 \times 10^{-4}$	76
6		790	$6.60 \times 10^{-6}$	905	15		720	$1.60 \times 10^{-4}$	63
7	650	820	$5.90 \times 10^{-4}$	17	16	650	515	$7.0 \times 10^{-6}$	942
8		770	$1.30 \times 10^{-4}$	72	17	615	850	$1.10 \times 10^{-4}$	103
9		720	$1.10 \times 10^{-4}$	99	18		820	$5.20 \times 10^{-5}$	172

The SEM fracture appearances of creep ruptured specimens at 600 and 650 under different stress levels are shown in Figure 2 and Figure 3, respectively. Typical intergranular brittle fracture and transgranular ductile fracture are observed from the SEM images. As the stress decreases, creep fracture mode converts from intergranular fracture to transgranular fracture.  $\sim 800$ MPa at 600 and  $\sim 700$ MPa at 650 are proved to be the critical conditions. Above this stress levels, the cavity nucleation, growth and coalescence into macrocracks along grain boundary result in the intergranular fracture mode. On the contrary, below this stress levels, the microstructural degradation leads to the decrease of matrix strength<sup>43</sup>. The stress concentration formed by the accumulation of dislocations at the particles results in the particle-matrix interface to experience the excess localized plastic deformation. This provides the sites for the nucleation of the cavities and the formation of the macrocracks, leading to transgranular fracture finally<sup>44</sup>. It can be observed that a mass of ductile dimples are formed, accompanied by prominent localized deformation (i.e. necking) as shown in Figure 2(K) and Figure 3(I, J, K).

#### Hosted file

image113.emf available at <https://authorea.com/users/417892/articles/575306-modeling-the-creep-deformation-and-damage-evolution-of-superalloy-gh4169-application-of-a-novel-damage-constitutive-model-based-on-continuum-damage-mechanics>

FIGURE 2 Fracture appearances of creep ruptured specimens at (A, E) 600/925MPa, (B, F) 600/880MPa, (C, G) 600/850MPa, (D, H) 600/820MPa, (I, J) 600/805MPa, and (K, L) 600/790MPa.

#### Hosted file

image114.emf available at <https://authorea.com/users/417892/articles/575306-modeling-the-creep-deformation-and-damage-evolution-of-superalloy-gh4169-application-of-a-novel-damage-constitutive-model-based-on-continuum-damage-mechanics>

FIGURE 3 Fracture appearances of creep ruptured specimens at (A, E) 650/820MPa, (B, F) 650/770MPa, (C, G) 650/720MPa, (D, H) 650/670MPa, (I, L) 650/615MPa, (J, M) 650/595MPa, and (K, N) 650/515MPa

### 5.2. Determination of the material constants

From Eq. and Eq., it can be determined that the constants needed to be obtained are  $\sigma_0$ ,  $n$ ,  $m$ ,  $\beta$ ,  $\gamma$ ,  $\delta$ , and  $\epsilon$ . The method to obtain those constants is described as follows:

#### 5.2.1. $\sigma_0$ and $n$

The ultimate tensile stress of 1440MPa and 1255MPa at 600 and 650 respectively, are determined by tensile tests. In order to determine the threshold stress, a standard linear extrapolation method was introduced by Mishra<sup>38,39</sup>, Huang<sup>40</sup> and Langdon<sup>45</sup> et al. And this method has been successfully used to determine the

threshold stress of Grade 91 steel<sup>46,47</sup>, ferritic-martensitic steel<sup>48</sup>, Fe-Cr-Ni alloy<sup>44</sup>, Grade 92 steel<sup>49</sup>, nickel-based superalloy<sup>50</sup>, etc. Using the same method, the threshold stresses at 600 and 650 were determined to be 593 MPa and 309 MPa in recent study<sup>28</sup>, respectively. It should be pointed out that the threshold stress is closely related to microstructural evolution and stability.

### 5.2.2. $\sigma_0$ , $n$ , and $m$

When damage is zero, Eq. (1) simplify to Eq. (2).  $E_a$  is the apparent activation energy of TTC relations, which can be calculated from the slop of diagram at constant  $\sigma$ .

Taking the logarithm of Eq. (1) and Eq. (2) gives:

Therefore, constants  $m$  and  $n$  are the slope and y-intercept in the — and — diagrams, respectively. Full details are given in reference [28].

### 5.2.3. $C_1$

To ensure when failure occurs, the definition of constant here is consistent with the definition of Haque<sup>20,21</sup>, i.e.  $C_1$ . Constant  $C_1$  is determined directly from the experimental data. It can be inferred that constant has dependence on stress and temperature.

### 5.2.4. $C_2$

So far, all constants have been determined except for constant  $C_2$ . As mentioned above, the constant can be determined by the least square fitting of experimental damage Eq. (1) and analytical damage Eq. (2). In this study, the constant is obtained by minimizing the constructed mean square error (MSE) function:

where  $D_a$  is the analytical damage,  $D_e$  is the experimental damage, and  $N$  is the number of test data.

In order to verify the interpolation and extrapolation abilities of the novel model, specimens 1-12 are used to calibrate the novel damage constitutive model. The obtained constants  $m$ ,  $n$ ,  $C_1$ ,  $C_2$ , and  $E_a$  are summarized in Table 3. The material constants  $m$  and  $n$  exhibit the dependence on stress and temperature. The constant  $E_a$  is determined directly using Eq. (2) experimentally. The constant  $C_1$  is determined by the least square fitting of experimental damage Eq. (1) and analytical damage Eq. (2). The calibrated constants  $C_2$  and  $E_a$  are listed in Table 4.

TABLE 3 Values of material constants

Constants				
Values	8.6249	1.8529	0.3602	-0.4244
Constants	$Q_N^*/\text{kJ/mol}$	/MPa	/MPa	—
Values	107.1	593(600) 309(650)	1440(600) 1255(650)	—

TABLE 4 The stress and temperature dependence of constants  $m$  and  $n$

No.	$\sigma$ / MPa	$T$ / MPa	$m$	$n$	No.	$\sigma$ / MPa	$T$ / MPa	$m$	$n$
1	600	925	5.4405	2.5231	7	650	820	5.9752	1.2514
2		880	6.3619	3.1661	8		770	5.2661	1.5197
3		850	7.2154	3.3452	9		720	7.8330	1.9829
4		820	8.3066	3.7364	10		670	7.8367	2.2629
5		805	8.2449	4.3825	11		615	8.5792	2.4346
6		790	9.1056	4.7851	12		595	10.0064	3.0152

## 5.3. Predictive ability of the novel damage constitutive model

The variation of minimum creep rate and rupture time with applied stress predicted by the novel damage

constitutive model (Eq. and Eq.) at different temperature are shown in Figure 4. The predictions are performed using experimental results of specimens 1-12. Post-audit validation indicates that all experimental data points fall near the prediction curve, and satisfactory interpolation and extrapolation abilities can be achieved by the novel model. Combined with the intergranular and transgranular fracture modes determined by the SEM fracture morphology, an approximate fracture mode split line is also delineated in Figure 4.

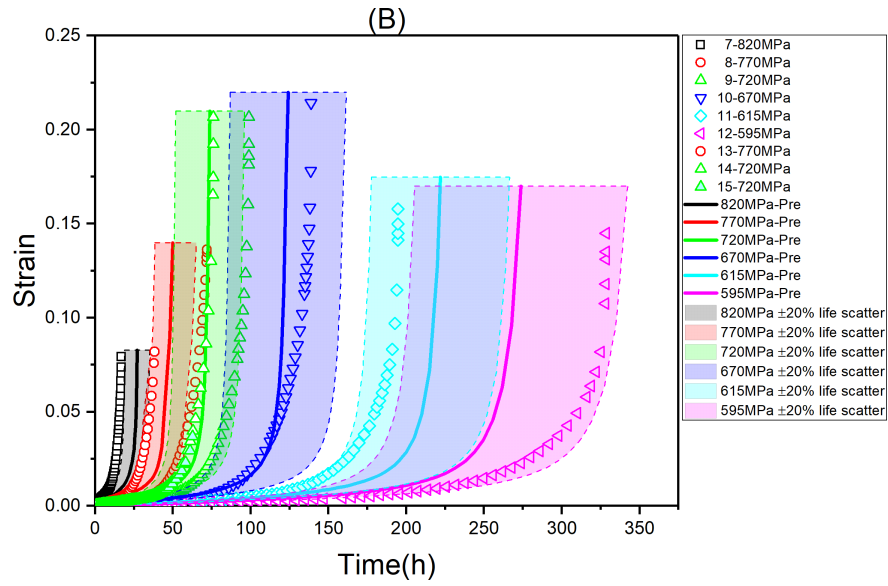
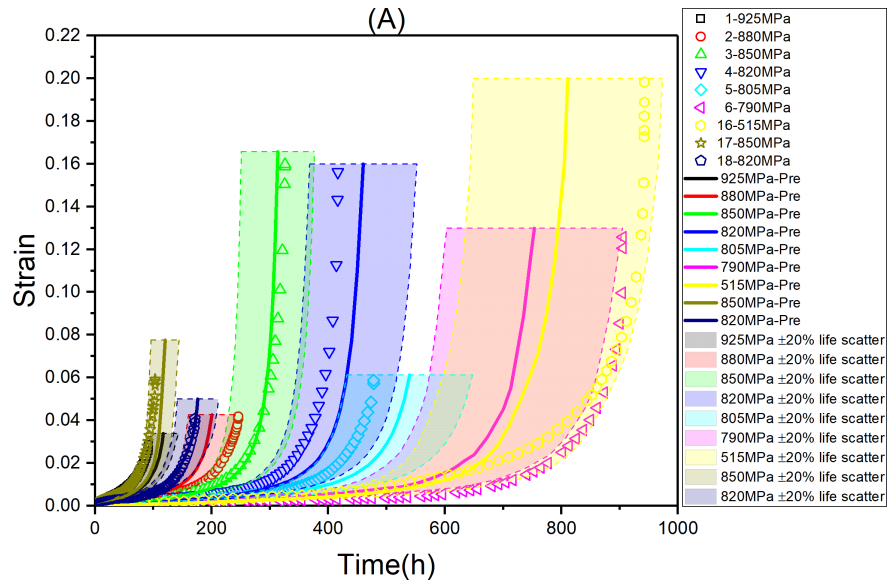
FIGURE 4 Predictions of (A) minimum creep rate and (B) rupture time.

After all constants are obtained, the damage evolution curve, i.e. Eq., can be determined by integrating Eq.. Theoretically, the creep strain curve can be obtained by integrating Eq. after introducing Eq. into it, i.e.

However, Eq. cannot be easily integrated to get a closed-form solution for creep deformation. Therefore, the fourth order Runge-Kutta method is adopted to obtain creep deformation curve, just like other researchers did previously<sup>6,17,36,51</sup>.

Creep deformation and damage evolution predicted by the novel damage constitutive model with experimental data are shown in Figure 5. When creep time reaches the rupture time, damage and failure occurs. The definition of constant makes the critical experimental damage always unity as shown in Figure 5C and Figure 5D. It can be seen that the prediction results of creep deformation and damage evolution almost fall in the scatter band, including the experimental results of interpolation and extrapolation. It is worth noting that the results of specimens 13-18 exhibited in Figure 5 rely on the stress and temperature dependence fitting function of constants and in Section 6.1 and Section 6.2. Essentially, CDM-based creep damage constitutive model is derived deterministically where scatter is not considered. The best fit line through the creep scattered data is the target of derivation. Then, the model can be calibrated to represent 50% reliability of deformation and damage. The scatter of creep data is inevitable, and this scatter can span across decades of creep rupture time in some cases. Since the CDM-based creep damage constitutive model cannot consider scatter, so the aim of the model is to model the average creep deformation and damage evolution under a certain condition, rather than focusing on fitting a single creep curve. This inherent property of the CDM-based damage constitutive model makes themselves have convincing extrapolation capability that classical plastic theory (CPT)-based model does not have, such as  $\vartheta$  projection method<sup>52</sup>.

To consider the scatter of creep data, some investigations have attempted to introduce stochastic processes into CDM-based creep damage constitutive model. Harlow presented a probabilistic K-R model which takes the uncertainty of model constants into account by using probability density function and probability theory<sup>53</sup>. Penny also proposed a probabilistic K-R model, and Monte Carlo simulation method was adopted to deal with the randomness of material and geometrical parameters<sup>54</sup>. Recently, Hossain and Steward have made a lot of efforts to simulate the uncertainty of creep deformation and damage evolution predicted by Sinh model where the randomness of material constants are achieved using Monte Carlo method and probability distribution function<sup>55-58</sup>.



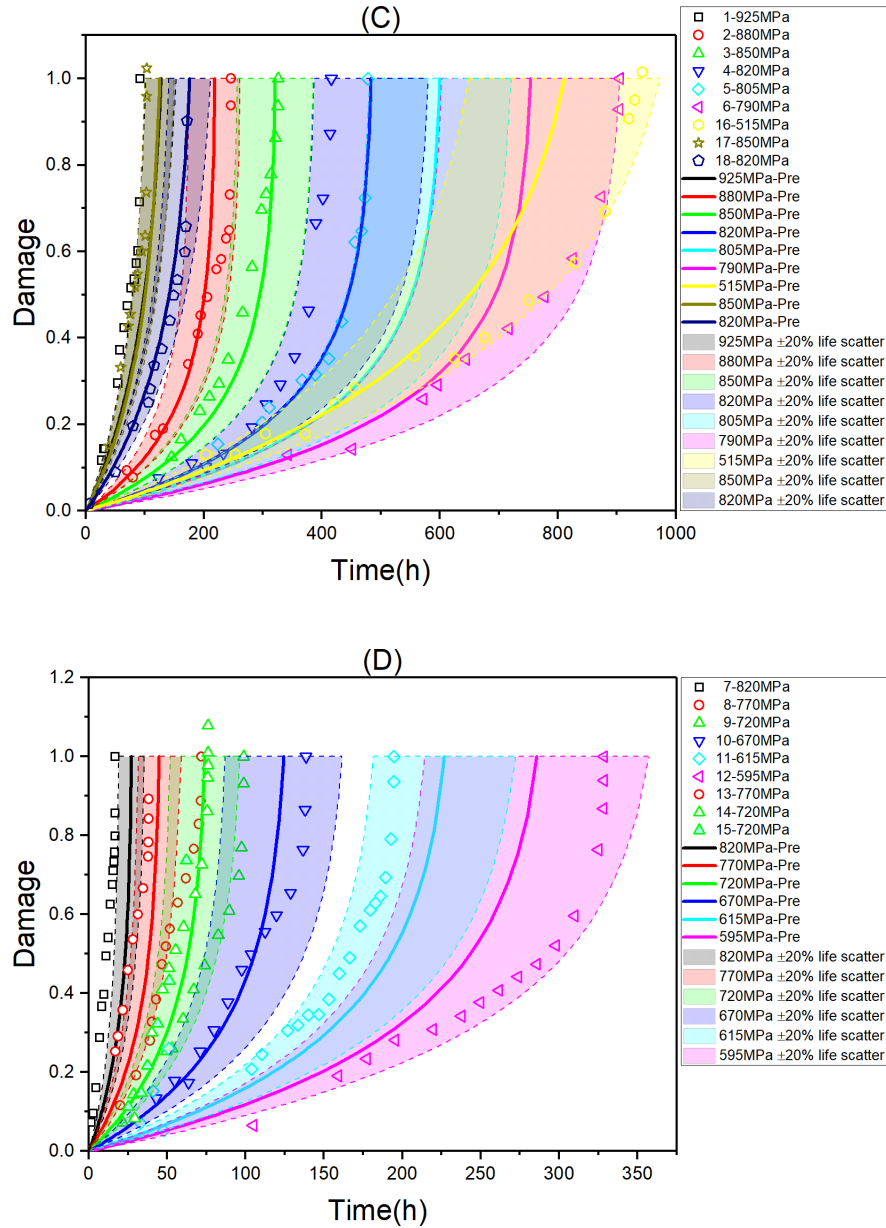


FIGURE 5 Creep deformation prediction of (A) specimens 1-6, 16-18, (B) specimens 7-15, and creep damage prediction of (C) specimens 1-6, 16-18, (D) specimens 7-15.

## 6. Discussion

### 6.1. The stress and temperature dependence of constant

To ensure experimental damage is unity when failure occurs, the constant is defined as  $\dot{\epsilon}$ . The constant shows the dependence on stress and temperature as described in Figure 6. With the decrease of stress, the constant increases. Cano<sup>23</sup> tried to use Eyring function to account for the stress dependence at a single temperature. However, Eyring function is not suitable to describe the co-dependence of constant on stress and temperature in this study. Hence, an empirical function is constructed as follows

where  $\dot{\epsilon}_0$ ,  $\sigma_0$ ,  $T_0$ , and  $\sigma_1$  are fitting constants. And above constants obtained by fitting constant of specimens 1-12 are

,,, Using this empirical function, the critical experimental damage values of specimens 13-18 are listed in Table 5. It can be observed that the critical experimental damage values are close to unity, which indicates that the selected empirical function is reasonable. After careful observation, the critical experimental damage value of specimen 15 is relatively far from unity, which can be attributed to the abrupt failure and lower rupture strain as shown in Figure 1.

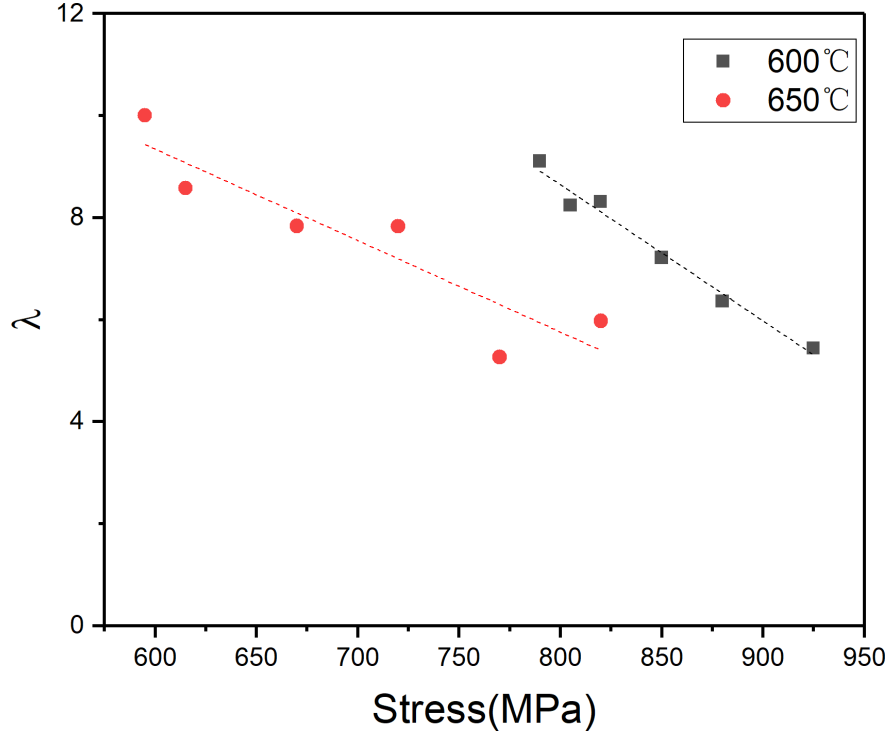


FIGURE 6 The stress and temperature dependence of constant .

TABLE 5 Critical experimental damage values of specimens 13-18.

No.	/	/MPa	Critical experimental damage values
13	650	770	0.8921
14	650	720	1.0785
15	650	720	0.7368
16	650	515	1.0149
17	615	850	1.0239
18	615	820	0.9021

## 6.2. Nonlinear creep damage accumulation effect

It can be seen from Table 4 that constant also exhibits the co-dependence on stress and temperature, which can be described in Figure 7 accordingly. Constant increases with the decrease of stress at a given temperature. Haque attributed the increase of to the accommodation of longer creep life<sup>22</sup>. However, according to Eq., constant controls the curvature of damage evolution curve, which means that the greater the constant , the greater the curvature of the damage evolution curve. In essence, the nonlinear creep damage

accumulation effect is revealed implicitly. The damage evolution with normalized time of specimens 1-12 under different stress at 600 and 650 are shown in Figure 8. Obviously, the nonlinear damage accumulation effect can be observed. A schematic diagram of nonlinear damage accumulation is shown in the Figure 9. For a two-step loading condition, if the specimen is firstly loaded at high stress level for normalized time , the damage will evolve from zero to point A. Subsequently, when low stress level condition is applied for normalized time up to failure, the damage will evolve from point A to point B horizontally, and finally reach to unity. In this case, the total life is reduced. This nonlinear damage accumulation effect has been evaluated quantitatively by using isodamage line theory for superalloy GH4169 in recent research<sup>59</sup>, i.e. the total life will be reduced when high stress condition was applied first. It should be pointed out that the opposing situation was also found for some other materials<sup>60</sup>. This means that the variation trend of the constant with stress can be essentially related to the different responses of the material to the load sequence effect.

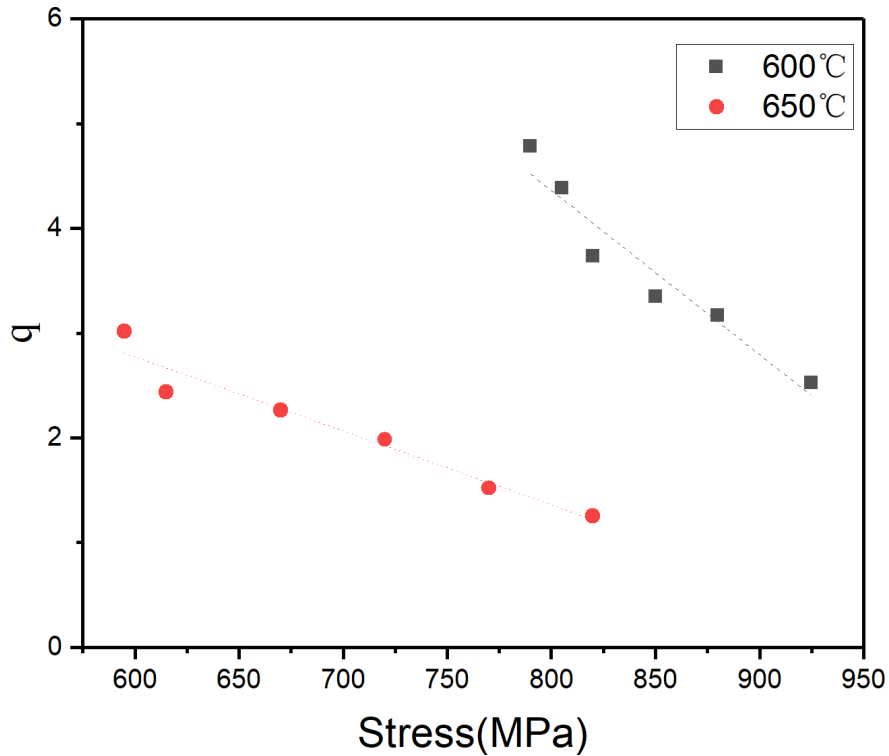


FIGURE 7 The stress and temperature dependence of constant  $q$ .

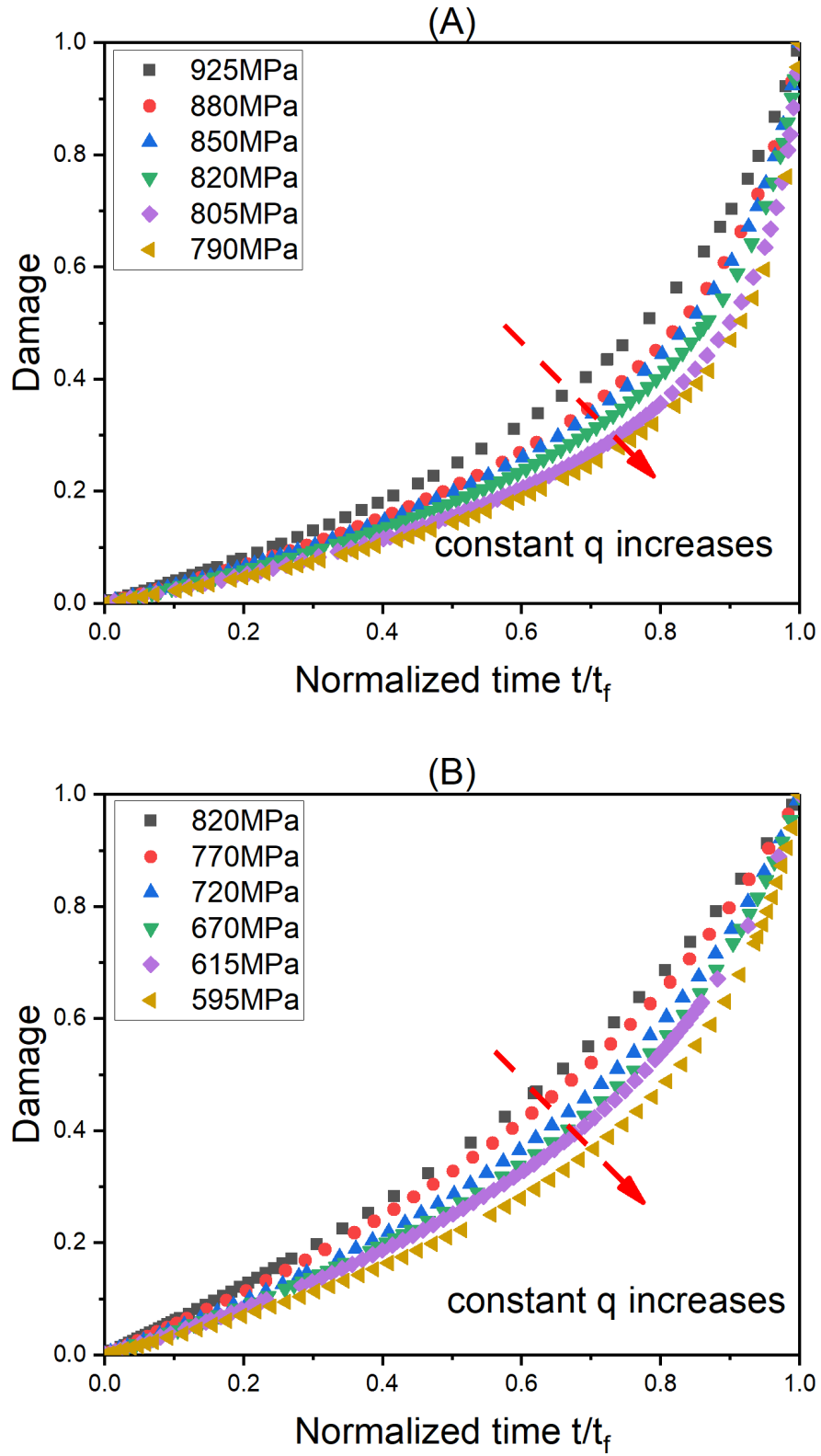


FIGURE 8 The evolution of damage with normalized time (A) at 600, and (B) at 650.

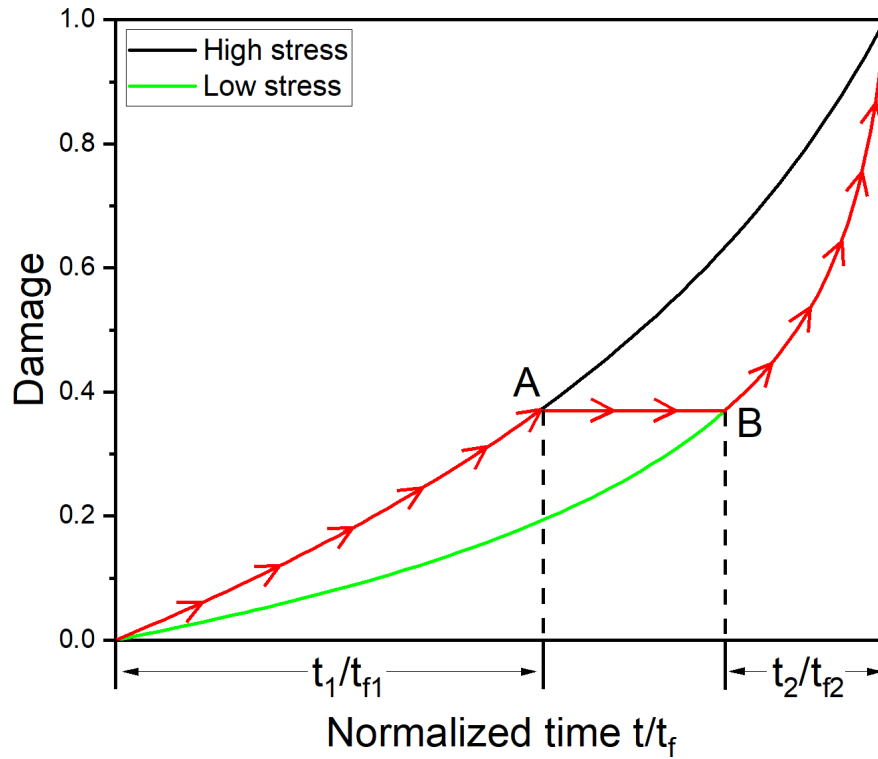


FIGURE 9 Schematic diagram of nonlinear damage accumulation.

Like constant, an empirical function is also constructed as follows:

where constants,  $\alpha$ ,  $\beta$ , and  $\gamma$  are obtained by best fitting. When the slope is zero,  $\alpha$  can be obtained, which means the slope is negative if  $\beta < 0$ . Constant  $\alpha$  will decrease with the increase of stress at a given temperature when the temperature is less than 727.

Eq. (1) can also be arranged as the function of temperature :

Similarly, when the slope is zero,  $\beta$  can also be calculated, which means the slope is negative if  $\alpha < 0$ . Constant  $\beta$  will decrease with the increase of temperature at a given stress when the stress is less than 1152MPa. Generally, the service temperature and stress of GH4169 are much lower than above ranges, which means that the total life will be reduced for those engineering structures made of GH4169 when high stress or high temperature loading condition is applied first.

## 7. Conclusion

In the present research, a novel damage constitutive model was proposed, which combined the TTC relations with continuum damage mechanics. The novel model overcame the disadvantages of power-law equation and Sinh equation that lack of explicit stress and temperature dependence of the constants, and satisfactory interpolation and extrapolation abilities were achieved. The conclusions of this work were as follows:

1. The novel model accurately predicted the minimum creep rate, rupture time, creep deformation and damage evolution process of GH4169.
2. The stress and temperature dependence of constants in the novel model were all determined, which overcame the disadvantages of the traditional CDM-based model and made the model have enough interpolation and extrapolation abilities.

3. Nonlinear creep damage accumulation effect of GH4169 was revealed from the aspect of continuum damage mechanism. Constant will decrease with the increase of stress or temperature, which means that the total life will be reduced when high stress or high temperature loading condition was applied first.

## Highlights

1. The novel model accurately predicts the minimum rate, rupture time, deformation and damage.
2. The novel model shows satisfactory interpolation and extrapolation abilities.
3. Fracture mode converts from intergranular to transgranular fracture as stress decreases.
4. Nonlinear creep damage accumulation effect is revealed by the novel model.

## Credit authorship contribution statement

**Xu Zhao:** Investigation, Methodology, Validation, Visualization. Writing - review & editing, Supervision, Project administration. **Xuming Niu:** Writing - original draft, Investigation, Methodology, Data curation. **Yingdong Song:** Validation, Project administration, Writing – review & editing, Supervision. **Zhigang Sun:** Supervision, Project administration, Writing – review & editing, Data curation.

## Acknowledgements

The authors would like to thank the National Science and Technology Major Project(J2019-V-0009-0103) and the Civil Aircraft Special Scientific Research Project(MJ-2018-D-25) for their support.

## Conflict of interest

The authors declare that they have no known competing financial interests or personal relationships that could have appeared to influence the work reported in this paper.

## Data availability statement

The raw/processed data required to reproduce these findings cannot be shared at this time as the data also forms part of an ongoing study.

## References

- 1 Song M, Xu T, Wang Q, et al. A modified theta projection model for the creep behaviour of creep-resistant steel. *Int J Press Vessel Pip* . 2018;165: 224–228.
- 2 Hong Y, Zhou C, Zheng Y, Zheng J, Zhang L, Chen X. Hydrogen effect on nanoindentation creep of austenitic stainless steel: A comparative study between primary creep stage and steady-state creep stage. *Int J Hydrogen Energy* . 2019;44: 22576–22583.
- 3 Liu X, Song L, Stark A, Lazurenko D, Pyczak F, Zhang T. Creep-induced  $\omega$  phase precipitation and cavity formation in a cast 45.5Ti-45Al-9Nb-0.5B alloy. *J Alloys Compd* . 2021;875: 160106.
- 4 Wang LY, Song ZM, Luo XM, Zhang GP. 3D X-ray tomography characterization of creep cavities in small-punch tested 316 stainless steels. *Mater Sci Eng A* . 2018;724: 69–74.
- 5 Hu JD, Xuan FZ, Liu CJ, Chen B. Modelling of cavity nucleation under creep-fatigue interaction. *Mech Mater* . 2021;156.
- 6 Dyson B. Use of CDM in materials modeling and component creep life prediction. *J Press Vessel Technol Trans ASME* . 2000;122: 281–296.
- 7 Kachanov LM. Time of the rupture process under creep conditions. *Time Rupture Process under Creep Cond* . 1958: 26–31.
- 8 Rabotnov YN. Creep problems in structural members. 1969.
- 9 Lemaitre J. *A Course on Damage Mechanics* . Springer Science & Business Media; 2012.

- 10 Chaboche J-L. Continuous damage mechanics—a tool to describe phenomena before crack initiation. *Nucl Eng Des* . 1981;64: 233–247.
- 11 Krajcinovic D. Damage mechanics: accomplishments, trends and needs. *Int J Solids Struct* . 2000;37: 267–277.
- 12 Murakami S. Continuum Damage Mechanics : A Continuum Mechanics Approach to the Analysis of Damage and Fracture. *Springer Ebooks* . 2012;41: 4731–4755.
- 13 Meng Q, Wang Z. Creep damage models and their applications for crack growth analysis in pipes: A review. *Eng Fract Mech* . 2019;205: 547–576.
- 14 Hyde TH, Ali BSM, Sun W. On the determination of material creep constants using miniature creep test specimens. *J Eng Mater Technol Trans ASME* . 2014;136.
- 15 Guo X, Gong J. An Improved Continuum Damage Constitutive Model for Creep. 2017: 1–9.
- 16 Saberi E, Nakhodchi S, Dargahi A, Nikbin K. Predicting stress and creep life in Inconel 718 blade-disk attachments. *Eng Fail Anal* . 2020;108: 104226.
- 17 C. Praveen, J. Christopher, V. Ganesan, G. V. Prasad Reddy, Shaju K. Albert. Prediction of Creep Behaviour of 316LN SS Under Uniaxial and Multiaxial Stress State Using Kachanov – Rabotnov Model at 923 K. *Trans Indian Inst Met* . 2020.
- 18 Wang X, Wang X, Zhu XZS. Creep damage characterization of UNS N10003 alloy based on a numerical simulation using the Norton creep law and Kachanov – Rabotnov creep damage model. *Nucl Sci Tech* . 2019;30: 1–9.
- 19 Haque MS. An Improved Sin-Hyperbolic Constitutive Model for Creep Deformation and Damage. 2015.
- 20 Haque MS, Stewart CM. A Novel Sin-Hyperbolic Creep Damage Model To Overcome the Mesh dependency of classic local approach Kachanov-Rabotnov model. In: *Proceedings of the ASME 2015 International Mechanical Engineering Congress and Exposition* . ; 2015:1–9.
- 21 Haque MS, Stewart CM. Comparison of a new sinhyperbolic creep damage constitutive model with the classic Kachanov-Rabotnov model using theoretical and numerical analysis. In: *TM2015 Annual Meeting Supplemental Proceedings* . ; 2015:937–945.
- 22 Haque MS, Stewart CM. Comparative analysis of the sin-hyperbolic and Kachanov – Rabotnov creep-damage models. *Int J Press Vessel Pip* . 2019;171: 1–9.
- 23 Cano JA, Stewart CM. A continuum damage mechanics (CDM) based Wilshire model for creep deformation, damage, and rupture prediction. *Mater Sci Eng A* . 2021;799.
- 24 Wilshire B, Battenbough AJ. Creep and creep fracture of polycrystalline copper. *Mater Sci Eng A* . 2007;443: 156–166.
- 25 Burt H, Wilshire B. Theoretical and practical implications of creep curve shape analyses for 7010 and 7075. *Metall Mater Trans A* . 2006;37 A: 1005–1015.
- 26 Wilshire B, Burt H, Lavery NP. Prediction of long term stress rupture data for 2124. *Mater Sci Forum* . 2006;519–521: 1041–1046.
- 27 Wilshire B, Scharning PJ. Long-term creep life prediction for a high chromium steel. *Scr Mater* . 2007;56: 701–704.
- 28 Xu Zhao, Xuming Niu, Yingdong Song, Zhigang Sun. Improvement of creep behavior prediction using threshold stress and tensile properties: Introduction of the TTC relations. *Metall Mater Trans A Phys Metall Mater Sci* . 2022: In production.

- 29 Zhao X, Niu X, Song Y, Sun Z. An investigation of the nonlinear creep damage accumulation of different materials: Application of a novel damage model. *Fatigue Fract Eng Mater Struct* . 2022;45: 530–545.
- 30 Hyde TH, Sun W, Tang A. Determination of material constants in creep continuum damage constitutive equations. *Strain* . 1998;34: 83–90.
- 31 Stewart CM, Gordon AP. Strain and damage-based analytical methods to determine the Kachanov-Rabotnov tertiary creep-damage constants. *Int J Damage Mech* . 2012;21: 1186–1201.
- 32 Stewart CM, Gordon AP. Analytical method to determine the tertiary creep damage constants of the Kachanov-Rabotnov constitutive model. *ASME Int Mech Eng Congr Expo Proc* . 2010;9: 177–184.
- 33 Murakami S, Liu Y, Mizuno M. Computational methods for creep fracture analysis by damage mechanics. *Comput Methods Appl Mech Eng* . 2000;183: 15–33.
- 34 liu Y, Murakami S. Damage localization of conventional creep damage models and proposition of a new model for creep damage analysis. *Int J Ser A* . 1998;41: 57–65.
- 35 Chang Y, Xu H, Ni Y, Lan X, Li H. The effect of multiaxial stress state on creep behavior and fracture mechanism of P92 steel. *Mater Sci Eng A* . 2015;636: 70–76.
- 36 Rouse JP, Sun W, Hyde TH, Morris A. Comparative assessment of several creep damage models for use in life prediction. *Int J Press Vessel Pip* . 2013;108–109: 81–87.
- 37 Haque MS, Stewart CM. The disparate data problem: The calibration of creep laws across test type and stress, temperature, and time scales. *Theor Appl Fract Mech* . 2019;100: 251–268.
- 38 Deshmukh SP, Mishra RS, Kendig KL. Creep behavior and threshold stress of an extruded Al-6Mg-2Sc-1Zr alloy. *Mater Sci Eng A* . 2004;381: 381–385.
- 39 Deshmukh SP, Mishra RS, Robertson IM. Investigation of creep threshold stresses using in situ TEM straining experiment in an Al-5Y2O3-10SiC composite. *Mater Sci Eng A* . 2010;527: 2390–2397.
- 40 Huang Y, Langdon TG. The creep behavior of discontinuously reinforced metal-matrix composites. *Jom* . 2003;55: 15–20.
- 41 Vojdani A, Farrahi GH, Mehmanparast A, Wang B. Probabilistic assessment of creep-fatigue crack propagation in austenitic stainless steel cracked plates. *Eng Fract Mech* . 2018;200: 50–63.
- 42 Zentuti NA, Booker JD, Bradford RAW, Truman CE. Correlations between creep parameters and application to probabilistic damage assessments. *Int J Press Vessel Pip* . 2018;165: 295–305.
- 43 Chamanfar A, Sarrat L, Jahazi M, Asadi M, Weck A, Koul AK. Microstructural characteristics of forged and heat treated Inconel-718 disks. *Mater Des* . 2013;52: 791–800.
- 44 Zhang Y, Jing H, Xu L, Zhao L, Han Y, Zhao Y. High-temperature deformation and fracture mechanisms of an advanced heat resistant Fe-Cr-Ni alloy. *Mater Sci Eng A* . 2017;686: 102–112.
- 45 Li Y, Langdon TG. Unified interpretation of threshold stresses in the creep and high strain rate superplasticity of metal matrix composites. *Acta Mater* . 1999;47: 3395–3403.
- 46 Shrestha T, Basirat M, Charit I, Potirniche GP, Rink KK, Sahaym U. Creep deformation mechanisms in modified 9Cr-1Mo steel. *J Nucl Mater* . 2012;423: 110–119.
- 47 Shrestha T, Basirat M, Charit I, Potirniche GP, Rink KK. Creep rupture behavior of Grade 91 steel. *Mater Sci Eng A* . 2013;565: 382–391.
- 48 Prakash P, Vanaja J, Reddy GVP, Laha K, Rao GVS. On the effect of thermo-mechanical treatment on creep deformation and rupture behaviour of a reduced activation ferritic-martensitic steel. *J Nucl Mater* . 2019;520: 65–77.

- 49 Alsagabi S, Shrestha T, Charit I. High temperature tensile deformation behavior of Grade 92 steel. *J Nucl Mater* . 2014;453: 151–157.
- 50 Huo JS, Gou JT, Zhou LZ, Qin XZ, Li GS. High temperature creep deformation mechanisms of a hot corrosion-resistant nickel-based superalloy. *J Mater Eng Perform* . 2007;16: 55–62.
- 51 Li LT, Lin YC, Zhou HM, Jiang YQ. Modeling the high-temperature creep behaviors of 7075 and 2124 aluminum alloys by continuum damage mechanics model. *Comput Mater Sci* . 2013;73: 72–78.
- 52 Evans RW, Wilshire B. *Creep of Metals and Alloys* . United States: IMM North American Pub. Center, Brookfield, VT; 1985.
- 53 Harlow DG, Delph TJ. A computational probabilistic model for creep-damaging solids. 1995;54: 161–166.
- 54 Penny RK, Weber MA. Robust methods of life assessment during creep. *Int J Press Vessel Pip* . 1992;50: 109–131.
- 55 Abir Hossain M, Stewart CM. Probabilistic minimum-creep-strain-rate and stress-rupture prediction for the long-term assessment of IGT components. In: *Proceedings of the ASME Turbo Expo* . Vol 10B-2020. ; 2020:1–11.
- 56 Hossain A, Stewart CM. A probabilistic creep model incorporating test condition , initial damage , and material property uncertainty. *Int J Press Vessel Pip* . 2021;193.
- 57 Hossain MA, Stewart CM. Reliability prediction of 304 stainless steel using sine-hyperbolic creep damage model with monte carlo simulation method. In: *American Society of Mechanical Engineers, Pressure Vessels and Piping Division (Publication) PVP* . Vol 6A-2019. ; 2019:0–10.
- 58 Hossain MA, Cano JA. Probabilistic Creep Modeling of 304 Stainless Steel Using a Modified Wilshire Creep-Damage Model. In: *Proceedings of the ASME 2020 Pressure Vessels & Piping Conference* . ; 2020:11.
- 59 Zhao X, Niu X, Song Y, Sun Z. An investigation of the nonlinear creep damage accumulation of different materials: Application of a novel damage model. *Fatigue Fract Eng Mater Struct* . 2021.
- 60 Pavlou DG. Creep life prediction under stepwise constant uniaxial stress and temperature conditions. *Eng Struct* . 2001;23: 656–662.

#### Hosted file

Figure.doc available at <https://authorea.com/users/417892/articles/575306-modeling-the-creep-deformation-and-damage-evolution-of-superalloy-gh4169-application-of-a-novel-damage-constitutive-model-based-on-continuum-damage-mechanics>

#### Hosted file

Table.docx available at <https://authorea.com/users/417892/articles/575306-modeling-the-creep-deformation-and-damage-evolution-of-superalloy-gh4169-application-of-a-novel-damage-constitutive-model-based-on-continuum-damage-mechanics>